

Formation and decay of vorticity in coupled helium-II flow

Olusola C. Idowu

University of Newcastle, Newcastle Upon Tyne, NE1 7RU, United Kingdom

Karen L. Henderson

University of the West of England, Bristol, BS16 1QY, United Kingdom

David C. Samuels

University of Newcastle, Newcastle Upon Tyne, NE1 7RU, United Kingdom

(Received 20 July 2000; published 20 December 2000)

The kinematic viscosity of helium II below the transition temperature can be defined with the total density of the liquid or the normal-fluid density alone. These two definitions have very different temperature dependences. In this work we considered the decay of Gaussian distributions of vorticity in helium II using the two fluid Hall-Vinen-Bekharevich-Khalatnikov equations. Our calculation shows that in these two-dimensional axisymmetric flows both fluids decay together with a viscous time scale set by the total fluid density and not by the normal-fluid density alone. We also considered the spin-up of each fluid and observed that for all initial conditions considered both fluids tend towards a matched vorticity state.

DOI: 10.1103/PhysRevB.63.024513

PACS number(s): 67.57.De, 47.37.+q

I. INTRODUCTION

Helium II at temperatures below the λ transition ($T_\lambda \approx 2.178$ K) can be described macroscopically by Landau's two-fluid model¹ as a superposition of a normal fluid with velocity \mathbf{v}_n and a superfluid with velocity \mathbf{v}_s . The circulation in the superfluid is quantized with a fixed value of $\kappa \approx 10^{-3}$ cm²/s. The normal-fluid component has a very small but nonzero viscosity μ_n and the superfluid has no viscosity. Each fluid has its own density, ρ_n and ρ_s for the normal fluid and superfluid respectively. The kinematic viscosity of helium II may be defined reasonably in two different ways, $\nu_n = \mu_n/\rho_n$ or $\nu = \mu/\rho$, where $\rho = \rho_n + \rho_s$ is the total density. The density of both fluids varies strongly with temperature,² hence these two definitions have different temperature dependences (Fig. 1). Since the normal-fluid and superfluid flows are coupled through mutual friction, it is not clear whether ν_n , ν , or another choice will best describe the coupled helium II flow.

One of the most generally accepted equations for modeling the macroscopic flow of helium II is the Hall-Vinen-Bekharevich-Khalatnikov (HVBK) equations.³⁻⁷ These equations generalize Landau's two-fluid equations¹ by taking into account the presence of quantized vortex lines in the flow. The derivation of the equations is based on a continuum approximation, assuming a high density of vortex lines locally aligned roughly in the same direction. The HVBK equations introduce two new physical effects which are absent from Landau's theory. First the mutual friction force which describes the scattering of rotons by the vortex lines and secondly the vortex tension force which results from the fact that the vortex lines have energy per unit length. Steady solutions of the HVBK equations have been found for a number of flows, for example solid body rotation inside a rotating cylinder,⁴ Couette flow between two infinitely long, concentric, rotating cylinders,⁸ and flow in a Couette annulus.⁹ In this paper, we used the HVBK equa-

tions to study the evolution of vorticity in helium II from various initial conditions in a cylindrical geometry.

We calculated the vorticity generated in both fluids using Gaussian distributions of vorticity as initial conditions. The Gaussian distribution of vorticity is a natural choice of initial condition since it is a simple solution for both the Navier-Stokes equation and the Euler equation. We have examined the development of strongly coupled two-fluid flows from various different initial conditions, and we have compared the decay rate for the vorticity distribution in this coupled helium II flow to the decay of vorticity in classical hydrodynamics.

Numerical calculations by Fiszdon, Peradzynski, and Poppe¹⁰ used a simplified HVBK model to consider the evolution of axisymmetric vortex systems in helium II taking Gaussian and top-hat profiles as initial vorticity distributions. They concluded that the evolution of the vorticity distributions varies primarily with the initial conditions, however their results are of limited practical interest since they neglected the viscosity of the normal-fluid in their calculations.

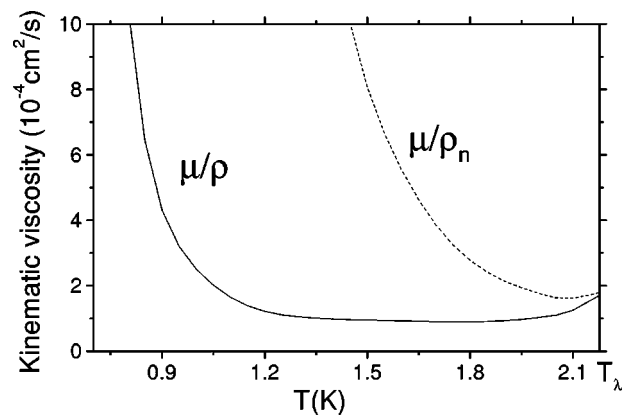


FIG. 1. Kinematic viscosity of liquid helium II using the T-90 values (Ref. 2).

Peradzynski, Filipkowski, and Fiszdon¹¹ considered the spin-up of helium II in both a finite and infinite axisymmetric cylinder by numerically time stepping another simplified HVBK model. They assumed that the flow within a spin-up cylinder has two regions; a region where the velocities of the two fluids are equal, and a region where the superfluid vorticity is zero. The implication of these two assumptions is that the mutual friction force is zero in both regions. We can gain a better understanding of evolution of vortices by solving the full HVBK equations including the viscous and mutual friction terms.

II. THE MODEL FLOW

We considered helium II contained within an infinitely long cylinder of radius R . We nondimensionalize the HVBK equations using R as the unit of length and R^2/ν_n , the normal-fluid viscous time scale, as the unit of time. Although R^2/ν_n is the natural choice for the time scale based on the form of the HVBK equations, we will show that the coupled flow actually scales with the viscous time scale set by R^2/ν . We considered flow configurations for both the normal fluid and superfluid such that the velocities are entirely in the azimuthal direction and depend on the dimensionless radial distance r only. Thus in cylindrical coordinates the computational domain is $0 \leq r \leq 1$ and the nondimensional velocity profiles may be expressed as $\mathbf{v}_n = v_n(r, t) \hat{\phi}$ and $\mathbf{v}_s = v_s(r, t) \hat{\phi}$. This leads to purely axial vorticity profiles for both fluids which may be written as $\boldsymbol{\omega}_s = \omega_s(r, t) \hat{z}$ and $\boldsymbol{\omega}_n = \omega_n(r, t) \hat{z}$.

Given these geometrical restrictions, we can write the nondimensional form of the HVBK equations as

$$\frac{\partial v_n}{\partial t} = \frac{\partial^2 v_n}{\partial r^2} + \frac{1}{r} \frac{\partial v_n}{\partial r} - \frac{v_n}{r^2} - \frac{B\rho_s}{2\rho} |\omega_s| (v_n - v_s), \quad (1)$$

$$\frac{\partial v_s}{\partial t} = \frac{B\rho_n}{2\rho} |\omega_s| (v_n - v_s), \quad (2)$$

where B is a temperature dependent mutual friction parameter.² Due to our choice of symmetry, the vortex tension term^{8,9} does not appear in this problem. In order to solve the above equations we need to impose boundary conditions. Both fluids must satisfy a regularity condition at the axis of the cylinder $r=0$ which will be incorporated into the solution method. Since the normal fluid is viscous it must satisfy the no-slip boundary condition at the wall of the cylinder, so we require that

$$v_n = 0 \text{ at } r = 1. \quad (3)$$

For the inviscid superfluid no such restriction is required, and the no-penetration boundary condition is automatically satisfied by the symmetry assumption for \mathbf{v}_s .

III. NUMERICAL METHOD OF SOLUTION

We solve Eqs. (1) and (2) together with the boundary condition, Eq. (3), using a spectral method.^{8,12} We expand v_n

and v_s over a truncated series of Chebychev polynomials

$$v_n(r, t) = \sum_{k=1}^N a_k^n(t) T_{2k-1}(r),$$

$$v_s(r, t) = \sum_{k=1}^N a_k^s(t) T_{2k-1}(r).$$

We have expanded over odd Chebychev polynomials only in order to satisfy the regularity condition at the axis of the cylinder. To solve for the normal-fluid spectral coefficients a_k^n , Eq. (1) is evaluated on r_k for $k=1, \dots, N-1$, where r_k are the positive zeroes of the $2N-2$ Chebychev polynomial of the second kind. To solve for the superfluid spectral coefficients a_k^s , Eq. (2) is evaluated on r_k for $k=1, \dots, N-1$ and also at the boundary point $r=1$. Crank-Nicholson is used on the linear terms while Adams-Bashforth is used on the nonlinear terms. Numerically, the problem reduces to solving the equation

$$\mathbf{A}\mathbf{a}^{[n+1]} = \mathbf{B}\mathbf{a}^{[n]} + \mathbf{f}^{[n, n-1]}, \quad (4)$$

where matrices \mathbf{A} and \mathbf{B} can be precomputed, $\mathbf{a}^{[n]}$ contains the spectral coefficients for the normal fluid and superfluid at the n th time step and \mathbf{f} contains the nonlinear terms. Given an initial profile we can time step the solution using

$$\mathbf{a}^{[n+1]} = \mathbf{A}^{-1} \mathbf{B}\mathbf{a}^{[n]} + \mathbf{A}^{-1} \mathbf{f}^{[n, n-1]}. \quad (5)$$

IV. INITIAL CONDITIONS

Using Eq. (5) we calculated the decay of Gaussian distributions of vorticity in both fluids. The Gaussian vorticity distribution is an exact solution of the Navier-Stokes equation and has a dimensionless vorticity distribution given by $\omega(r, t) \hat{z}$ with

$$\omega(r, t) = \frac{\Gamma}{\pi r_c^2(t)} \exp[-r^2/r_c^2(t)], \quad (6)$$

where Γ is the total circulation and $r_c(t)$ is the core radius. The corresponding velocity distribution is $v(r, t) \hat{\phi}$ with

$$v(r, t) = \frac{\Gamma}{2\pi r} \{1 - \exp[-r^2/r_c^2(t)]\}. \quad (7)$$

We begin each simulation with a Gaussian distribution in both the normal fluid and the superfluid vorticities. The initial circulations Γ_n and Γ_s and the initial core radii $r_{c,n}$ and $r_{c,s}$ may be equal in the two fluids, or may be different, depending on the specific case that we wish to examine.

With this definition, the vorticity is concentrated near the axis or the core of the cylinder and decreases with the radius. Assuming a Gaussian vortex as an initial velocity profile for the superfluid vorticity is equivalent to assuming that there is a high density of vortex lines all aligned axially and concentrated close to the axis of the cylinder. Previous numerical

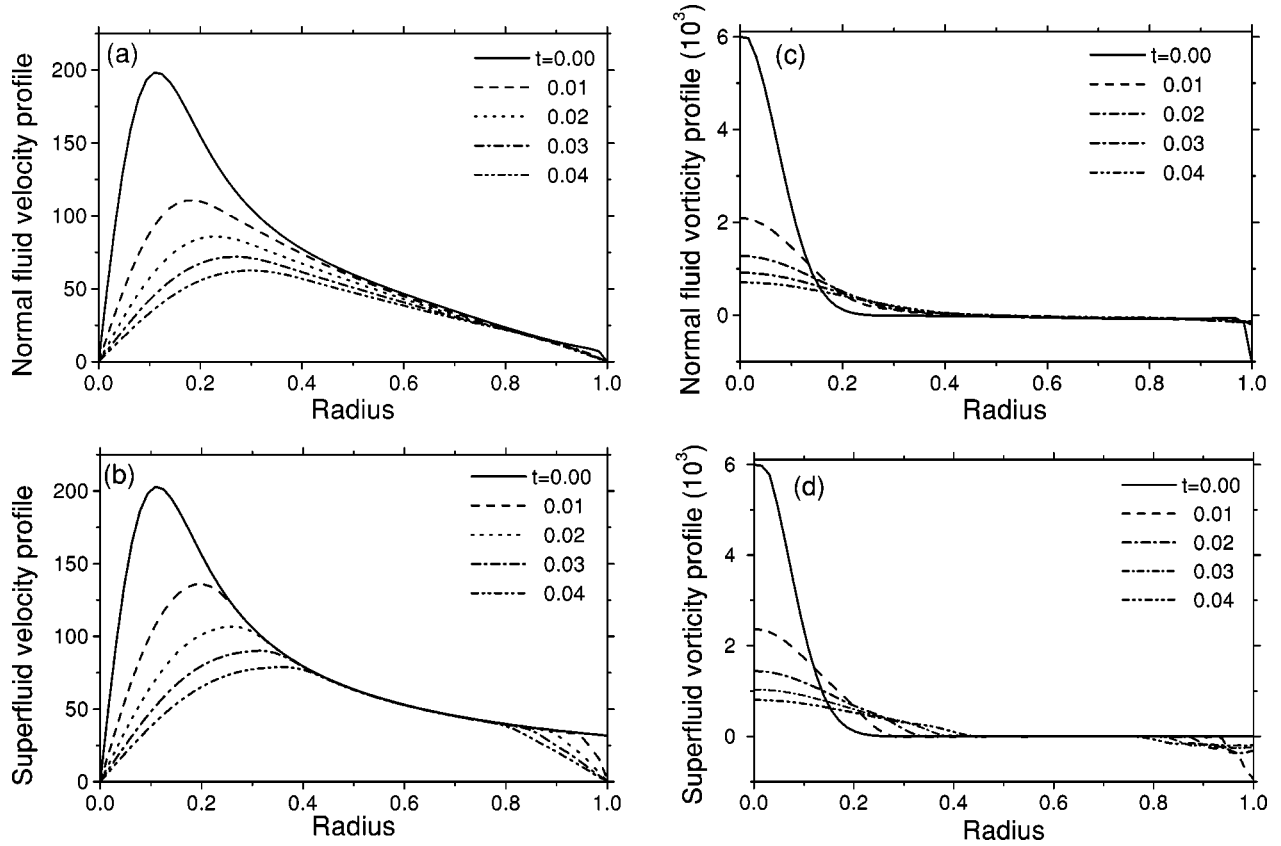


FIG. 2. Evolution of the normal-fluid and superfluid flows at $T = 1.9$ K. Starting with $\Gamma_s = \Gamma_n = 200$ and $r_{c,s} = r_{c,n} = 0.1$. (a) Normal-fluid velocity, (b) superfluid velocity, (c) normal-fluid vorticity, (d) superfluid vorticity.

work by Samuels¹³ shows that in helium II, vorticity in the superfluid is concentrated in the core of the normal-fluid Gaussian vortex.

The core radius of a classical decaying Gaussian vortex in a viscous fluid expands at the rate

$$r_c^2(t^*) = r_c^2(0) + 4t^*, \quad (8)$$

where t^* is the viscous time scaled with the fluid density ρ . The inverse peak vorticity for a decaying Gaussian vortex in a viscous fluid can be written as

$$\omega^{-1}(0, t^*) = \omega^{-1}(0, 0) + \frac{4\pi t^*}{\Gamma}. \quad (9)$$

We will use these classical results as tests of the effective viscosity for the decay of the coupled superfluid–normal-fluid system.

The viscous normal-fluid must satisfy the no-slip boundary condition, Eq. (3). To satisfy this condition we have taken an initial profile for the normal-fluid of the form

$$v_n = f(r)v, \quad (10)$$

where v is as in Eq. (7) and $f(r)$ is the weighting function

$$f(r) = \frac{0.5[1 - \tanh(4r - 3.4)] - A_1}{A_2}, \quad (11)$$

where $A_1 = 0.5[1 - \tanh(0.6)]$, ensuring that $f(1) = 0$ and thus the no-slip condition is satisfied and $A_2 = 0.5[\tanh(0.6) + \tanh(3.4)]$, ensuring that $f(0) = 1$. Thus taking an initial normal-fluid velocity profile of this form we have a Gaussian profile for the normal fluid vorticity close to the origin and yet the normal fluid satisfies the no-slip boundary condition at $r = 1$. The effect of the weighting function $f(r)$ is only strong in the region $0.9 < r \leq 1.0$

V. DECAY OF MATCHED GAUSSIAN VORTICES

Starting with initially matched Gaussian vorticity distributions (except near the boundary) for both fluids, the velocity distributions in both fluids decay [Figs. 2(a)–2(b)]. The velocity profile in the normal fluid decays differently from that of the superfluid profile. The superfluid velocity profile, in the radius interval $0.4 < r < 0.7$ decays much slower than does the normal-fluid profile [Fig. 2(b)].

The normal-fluid velocity maintained the no-slip boundary condition at the boundary for all time while the slip boundary condition in the superfluid velocity was quickly driven towards effectively a no-slip boundary condition via the mutual friction force. The initial velocity difference in both fluids at the boundary causes a large mutual friction force on the superfluid which generates a local concentration of negative vorticity (in comparison to the positive vorticity at $r = 0$). The magnitude of the negative vorticity grows until $v_s \rightarrow 0$ at $r = 1$. Then the mutual friction force is zero and the

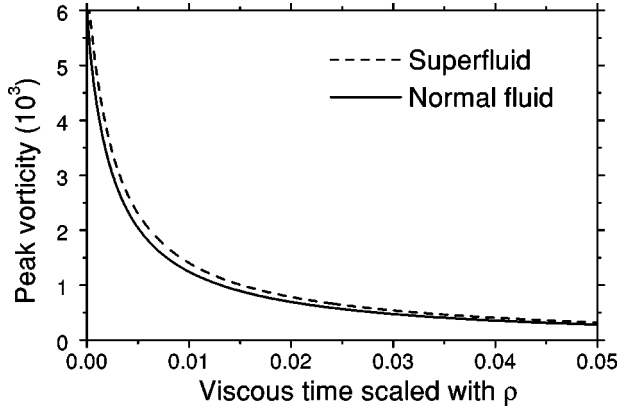


FIG. 3. Decay of peak vorticity in the normal-fluid and superfluid at $T=1.9$ K. Starting with $\Gamma_s=\Gamma_n=200$ and $r_{c,s}=r_{c,n}=0.1$.

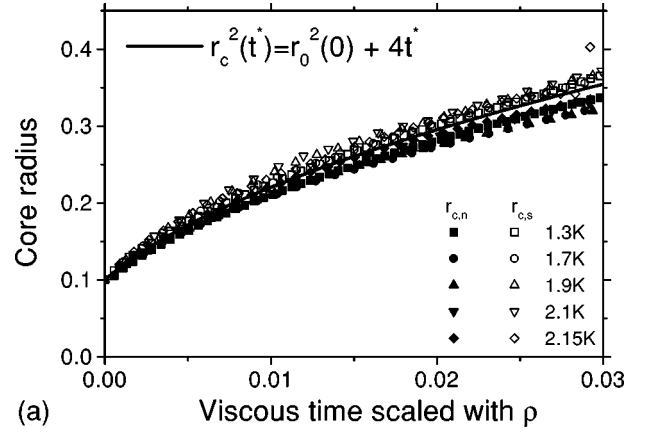
growth of the negative vorticity ends. Note that we never imposed a no-slip boundary condition on the superfluid, but the superfluid velocity was driven very nearly to zero at the boundary by the mutual friction force.

The effect of the mutual friction force varies at different radial positions. Equations (1) and (2) show that the mutual friction force is small when $v_n \approx v_s$ or when $\omega_s \approx 0$. There is a strong mutual friction effect at the boundary because of the velocity difference, and very little mutual friction effect in the radius interval $0.4 < r < 0.7$ because $\omega_s \approx 0$ at all times in this interval [Fig. 2(d)].

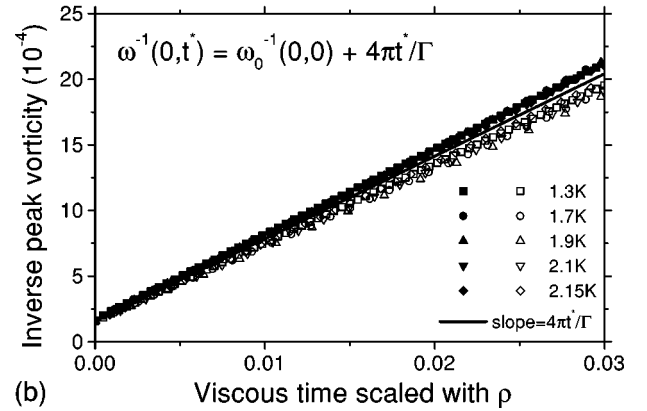
The peak vorticities in the normal fluid $\omega_n(r=0)$ and superfluid $\omega_s(r=0)$ decay exponentially in time (Fig. 3). The decay of the normal fluid is always ahead of the decay of the superfluid. The close similarity in the decay rate is counter intuitive because the decay mechanisms in Eqs. (1) and (2) represent different physical processes of decay. The normal-fluid flow decays through the usual viscous dissipation of energy. The superfluid flow, on the other hand, decays by transferring energy to the normal fluid through the mutual friction force. These different physical processes came to a balance so that both vorticity fields decay with similar rates.

The core radii $r_{c,n}$ and $r_{c,s}$ were defined at the radius where $\omega(r_c, t) = \omega(0, t)/e$, and were defined separately for each fluid. The core radii of both fluids expand in time at slightly different rates. However, when the core radii are plotted against the viscous time scaled with the total density, the radii are approximately equal [Fig. 4(a)], though clearly not identical. Similarly, the inverse peak vorticities in both fluids $\omega_n^{-1}(0, t)$ and $\omega_s^{-1}(0, t)$ scaled well with the time scale set by the total density of the fluid [Fig. 4(b)]. This shows that both fluids decay in a similar fashion with a time scale defined by total density of the fluid ρ . Recent experimental observations by Stalp *et al.*¹⁴ on the decay of superfluid turbulence also see this behavior, but it must be remembered that our model geometry is very simple in comparison to any turbulent flow.

The time dependence of the core radius of the classical decaying Gaussian vortex [Eq. 8], is very similar to that of the core radii of both the normal fluid and the superfluid



(a)



(b)

FIG. 4. (a) Expansion of the superfluid and normal-fluid core radius at $T=1.9$ K. Starting with $\Gamma_s=\Gamma_n=200$ and $r_{c,s}=r_{c,n}=0.1$. (b) Inverse vorticity at $r=0$, for different temperatures. Starting with $\Gamma_s=\Gamma_n=200$ and $r_{c,s}=r_{c,n}=0.1$.

[Fig. 4(a)]. Similarly, the inverse peak vorticity of the classical Gaussian vortex [Eq. (9)], compares well with the inverse peak vorticity in both fluids [Fig. 4(b)]. From this we can conclude that although the flows in the two fluids might decay due to different physical effects, the combined evolution of the two fluids behaves very much like a single classical fluid with one density ρ .

Although the peak vorticity in both fluids are close to each other, the ratio of the two peak vorticities $\omega_n(0, t)/\omega_s(0, t)$, and the peak velocities $v_n(r_{c,n}, t)/v_s(r_{c,s}, t)$ remain constant after the initial transient [Figs. 5(a) and 5(b), respectively] with values slightly less than 1. We chose these particular radii as measurement points because the peak vorticities occurred at $r=0$ and the peak velocities occurred at approximately $r=r_c$. As the coupled flow viscously decays the peak vorticity and peak velocity in the superfluid are always greater than those of the normal fluid and a constant ratio is maintained throughout the decay. We do not have a theoretical understanding for this steady behavior. The slight temperature dependence of the steady velocity ratio is plotted in Fig. 6(a). The steady vorticity ratio is plotted in Fig. 6(b). Both steady values have a minimum ratio at a temperature of approximately 1.9 K. At this temperature the densities of both fluids are approximately equal.

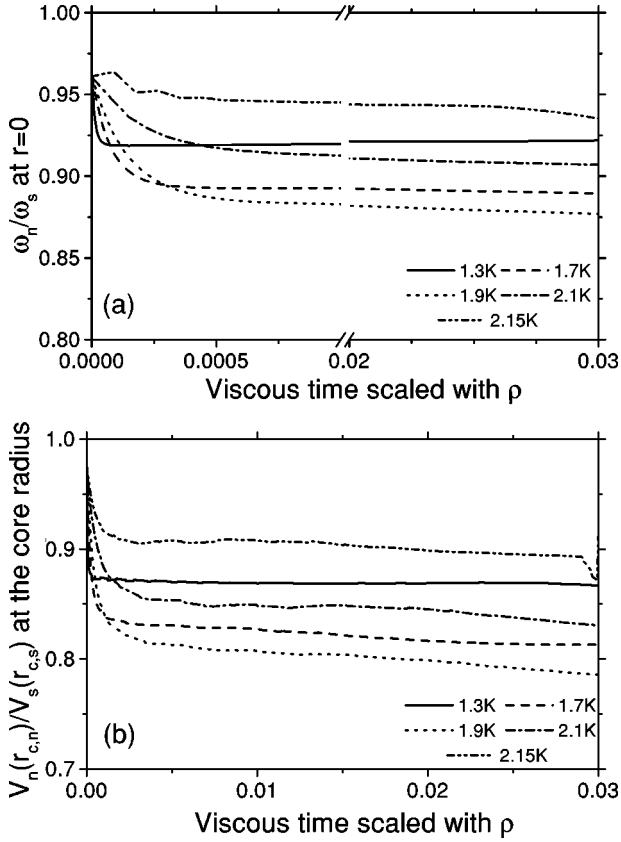


FIG. 5. (a) The development of the ratio of normal-fluid vorticity to superfluid vorticity at $r=0$ for different temperatures. Starting with $\Gamma_s=\Gamma_n=200$ and $r_{c,s}=r_{c,n}=0.1$. (b) Ratio of normal-fluid velocity and superfluid velocity at $r=r_c$ for different temperatures for the same initial conditions as in (a). After a scaled time of 0.03, the vorticities and velocities in both fluids become small enough that significant noise develops in both the vorticity and velocity ratios.

VI. THE SPIN-UP PROBLEM

We considered the spin-up of a seed of normal-fluid vorticity in the presence of a Gaussian distribution of vorticity in the superfluid. The small seed used in the normal fluid has a small Gaussian distribution of vorticity with a peak vorticity of approximately 1% compared to the initial peak vorticity in the superfluid. The superfluid decays initially by transferring energy to the normal fluid [Fig. 7(a)]. The normal fluid then starts to decay after its initial growth, before a matched vorticity state can be achieved. The vorticity in the superfluid is always slightly higher than the vorticity in the normal fluid throughout the decay process. Simulations starting with a small negative seed of vorticity (of opposite sign to ω_s) developed to a matched vorticity state in almost exactly the same manner as the positive seed simulations. This is expected from the form of Eq. (1), confirming that the development of the matched vorticity state by the spin-up of the normal fluid is independent of the initial state of the normal fluid, as long as $|\omega_s| \gg |\omega_n|$ in the initial state.

The initial growth in the normal-fluid vorticity can be roughly estimated from Eqs. (1) and (2). Taking the curl of

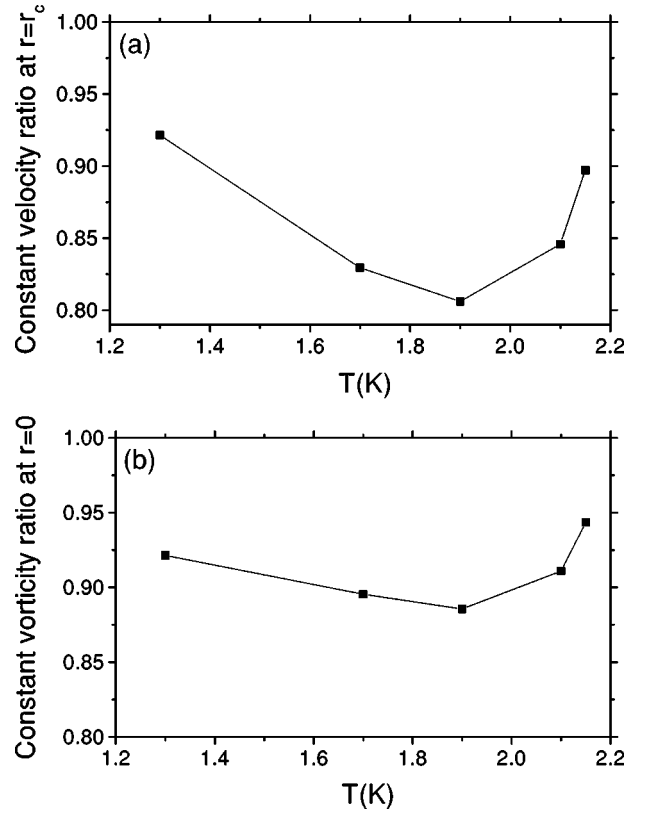


FIG. 6. (a) Steady velocity ratio at $r=r_c$. (b) Steady vorticity ratio at $r=0$.

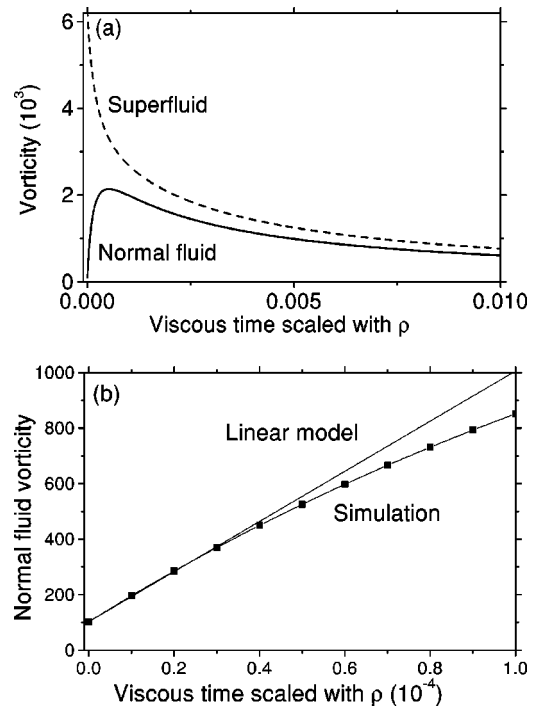


FIG. 7. Spin-up of the normal-fluid at $T=1.9$ K, starting with $\Gamma_s=200$ and $\Gamma_n=2$. (a) Evolution of the peak normal fluid and superfluid vorticity. (b) Initial growth of the peak normal-fluid vorticity.

$\partial \mathbf{v}_n / \partial t$ and $\partial \mathbf{v}_s / \partial t$, from Eqs. (1) and (2), respectively, we have

$$\frac{\partial \omega_n}{\partial t} = \left(\frac{\partial^2 \omega_n}{\partial r^2} + \frac{1}{r} \frac{\partial \omega_n}{\partial r} \right) - \frac{B\rho_s}{2\rho} \left(|\omega_s|(\omega_n - \omega_s) + (v_n - v_s) \frac{\partial |\omega_s|}{\partial r} \right), \quad (12)$$

$$\frac{\partial \omega_s}{\partial t} = \frac{B\rho_n}{2\rho} \left(|\omega_s|(\omega_n - \omega_s) + (v_n - v_s) \frac{\partial |\omega_s|}{\partial r} \right). \quad (13)$$

Suppose that the initial growth in the normal fluid occurs while $\omega_s(0,t)$ is approximately constant. Then the initial growth for the normal fluid [for $\omega_s(0,t) \gg \omega_n(0,t)$] from Eq. (12) can be written as

$$\begin{aligned} \omega_n &= \omega_n(0,t) \exp\left(-\frac{B\rho_s}{2\rho} \omega_s(0,t)t\right) \\ &+ \omega_s(0,t) \left[1 - \exp\left(-\frac{B\rho_s}{2\rho} \omega_s(0,t)t\right) \right] \\ &\approx \omega_n(0,t) + \frac{B\rho_s}{2\rho} \omega_s^2(0,t)t. \end{aligned} \quad (14)$$

This linear approximation is only valid for $t \ll 2\rho/B\rho_s\omega_s(0,t)$. The linear growth is compared to the simulation in Fig. 7(b).

Similarly we computed the spin-up of a small seed of superfluid vorticity in the coupled flow. The small seed used is a Gaussian vorticity distribution with a peak vorticity of approximately 1% of the normal-fluid peak vorticity. The spin-up process for the superfluid is different from that of the normal fluid discussed in the previous paragraph [Fig. 8(a)]. The superfluid gains vorticity from the normal fluid through the mutual friction coupling until it grows past the normal-fluid vorticity. Then ω_s starts to decay by transferring vorticity back to the normal fluid which then loses the vorticity through viscous dissipation.

The initial growth of the superfluid vorticity can be calculated from Eq. (13) if we assume that $\omega_n(0,t)$ is approximately constant during the initial growth and $\omega_n(0,t) \gg \omega_s(0,t)$. Then the superfluid vorticity is

$$\begin{aligned} \omega_s &= \frac{\omega_n(0,t) \omega_s(0,t) \exp\left[\frac{B\rho_n}{2\rho} \omega_n(0,t)t\right]}{\omega_n(0,t) - \omega_s(0,t) \left\{ 1 - \exp\left[\frac{B\rho_n}{2\rho} \omega_n(0,t)t\right] \right\}} \\ &\approx \omega_s(0,t) \exp\left(\frac{B\rho_n}{2\rho} \omega_n(0,t)t\right). \end{aligned} \quad (15)$$

The comparison of this growth with the simulation is shown in Fig. 8(b).

For both the spin-up of the superfluid by the normal fluid, and the reverse, the vorticity always goes towards a matching state, and then the nearly matched vorticity distributions decay together. During the decay of the nearly matched flow

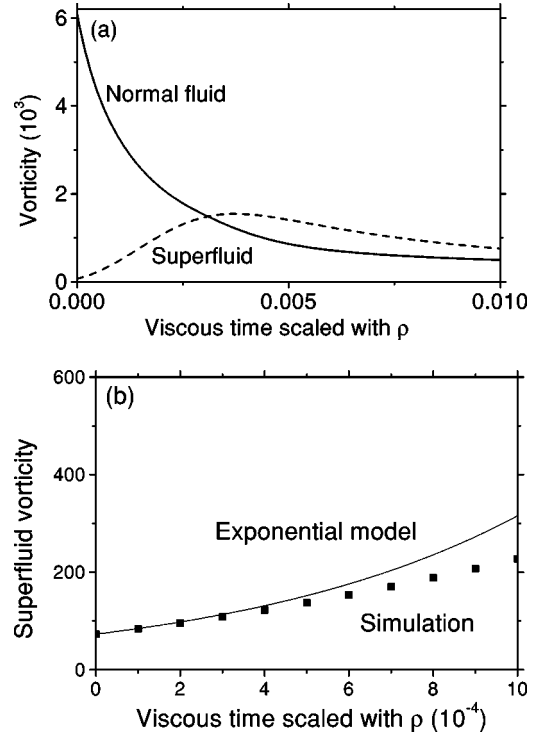


FIG. 8. Spin-up of the superfluid at $T=1.9$ K, starting with $\Gamma_s = 2$ and $\Gamma_n = 200$. (a) Evolution of the peak superfluid and normal-fluid vorticity. (b) Initial growth of the peak superfluid vorticity.

we always find that the superfluid vorticity has a higher magnitude than the normal-fluid vorticity.

We also considered the evolution of a small negative seed of vorticity in the superfluid together with a positive Gaussian distribution of vorticity in the normal fluid. The small negative seed of vorticity in the superfluid was driven to zero everywhere in a very short time and we never observed a large scale superfluid vorticity structure developing in this case.

The generation of superfluid vorticity is of particular fundamental interest. We must remember that the superfluid vorticity field in the HVBK equations is a continuum approximation and that superfluid vorticity can actually only exist in the form of quantized vortex filaments. Thus any increase in the superfluid vorticity field ω_s must correspond to either the creation of new vortex filaments (known as the nucleation problem) or the movement of existing vortex filaments. One of the considerations taken into account in deriving the HVBK equations is that the superfluid circulation must be conserved,⁷ and the spin-up of the superfluid in these simulations represents the generation of new superfluid vortex filaments at the boundary, which are then transported by mutual friction through the interior.

VII. DISCUSSION

These calculations show that axisymmetric vorticity concentrations in helium II naturally prefer to *lock*. That is, they tend toward a matched vorticity state for a wide range of initial conditions. As long as there is at least a small seed of

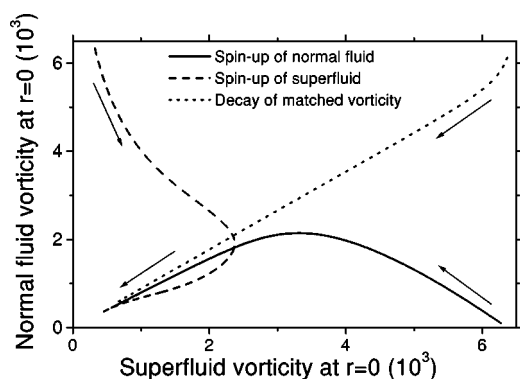


FIG. 9. Evolution of the normal-fluid and superfluid vorticity starting from different initial conditions.

superfluid vorticity aligned with the normal-fluid vorticity, then the normal-fluid vorticity will spin-up the superfluid. Conversely, a concentration of superfluid vorticity will spin-up the normal fluid to a matching rotation, without the need of any particular sign of seed vorticity in the normal fluid. Figure 9 shows the evolution of both the superfluid and the normal fluid vorticity at $r=0$ in both fluids starting from different initial conditions. The coupled flow system naturally develops to a state where the superfluid and normal-fluid vorticities are very close in magnitude, but not exactly equal. We typically see that the coupled flow develops so that the superfluid vorticity is slightly higher than the normal fluid vorticity.

The spin-up of the superfluid by the normal fluid has been seen before in simulations of superfluid vortex filament dynamics^{13,15} but these simulations treated the normal-fluid flow as fixed and thus were not calculations of the truly

coupled flow. These earlier simulations could not determine the flow that develops in the normal fluid, or deal with the viscous decay of the coupled flow. We find that the decay scale for the coupled motion of the two fluids is set by the total density of the fluid and not by the normal-fluid density alone. This behavior is observed for the flow of helium II throughout the temperature range examined $1.3 \text{ K} \leq T \leq 2.15 \text{ K}$. We find that the locking together of the vorticity fields of the two fluids is not strongly dependent on the relative densities of the two fluids, since these densities are strongly temperature dependent in this range. Though certainly the final values of vorticity reached in the locked state are strongly temperature dependent just due to energy limitations, the process of vorticity locking occurs throughout this temperature range.

The results presented here are for a specific geometry with high symmetry. Certainly the coupled turbulent flow will be much more complicated than that presented here, and may include behaviors that cannot occur in this geometry, or which may depend on the motion and instabilities of individual superfluid vortex filaments. But the basic process of vorticity matching described here is likely, in our opinion, to play an important role in any coupled flow of the normal fluid and superfluid. With this in mind, we believe the results presented in this paper further clarify and extend our understanding of experiments on turbulence in helium II.

ACKNOWLEDGMENTS

This research was supported by University of Newcastle upon Tyne and the University of the West of England. K.L.H. gratefully acknowledges the support of Nuffield Foundation.

¹ L.D. Landau and E.M. Lifshitz, *Fluid Mechanics* (Pergamon, New York, 1987).

² R.J. Donnelly and C.F. Barenghi, *J. Phys. Chem. Ref. Data* **27**, 1217 (1998).

³ H.E. Hall and W.F. Vinen, *Proc. R. Soc. London, Ser. A* **238**, 215 (1956).

⁴ H.E. Hall, *Philos. Mag. Suppl.* **9**, 89 (1960).

⁵ I.M. Khalatnikov, *An Introduction to the Theory Superfluidity* (Benjamin, New York, 1956).

⁶ R.J. Donnelly, *Quantized Vortices in Helium II* (Cambridge University Press, Cambridge, 1991).

⁷ R.N. Hills and P.H. Roberts, *Arch. Ration. Mech. Anal.* **66**, 43 (1977).

⁸ K.L. Henderson, C.F. Barenghi, and C.A. Jones, *J. Fluid Mech.*

283, 329 (1995).

⁹ K.L. Henderson and C.F. Barenghi, *J. Fluid Mech.* **406**, 199 (2000).

¹⁰ W. Fiszdon, Z. Peradzynski, and W. Poppe, *Phys. Fluids* **28**, 3525 (1985).

¹¹ Z. Peradzynski, S. Filipkowski, and W. Fiszdon, *Eur. J. Mech. B/Fluids* **9**, 259 (1990).

¹² K.L. Henderson and C.F. Barenghi, *J. Low Temp. Phys.* **98**, 351 (1995).

¹³ D.C. Samuels, *Phys. Rev. B* **47**, 2107 (1993).

¹⁴ S.R. Stalp, L. Skrbek, and R.J. Donnelly, *Phys. Rev. Lett.* **82**, 4831 (1998); S.R. Stalp, J.J. Niemela, and R.J. Donnelly, *Physica B* **284**, 75 (2000).

¹⁵ C.F. Barenghi, D.C. Samuels, G.H. Bauer, and R.J. Donnelly, *Phys. Fluids* **9**, 2631 (1997).